High ATP6V1B1 expression is associated with poor prognosis and platinum-based chemotherapy resistance in epithelial ovarian cancer

GWAN HEE HAN[1], HEE YUN[2], JOON-YONG CHUNG[3], JAE-HOON KIM[4,5] and HANBYOUL CHO[4,5]

[1]Department of Obstetrics and Gynecology, Sanggye Paik Hospital, Inje University College of Medicine, Seoul 01757;
[2]Department of Obstetrics and Gynecology, Gangnam Severance Hospital, Yonsei University College of Medicine,
Seoul 06299, Republic of Korea; [3]Molecular Imaging Branch, Center for Cancer Research, National Cancer Institute,
National Institutes of Health, Bethesda, MD 20892, USA; [4]Department of Obstetrics and Gynecology,
Yonsei University College of Medicine, Seoul 06299; [5]Institute of Women's Life Medical Science,
Yonsei University College of Medicine, Seoul 03722, Republic of Korea

Abstract. The vacuolar ATPase H+ transporting V1 subunit B1 (ATP6V1B1) belongs to the family of ATP6Vs, which functions to transport hydrogen ions. The expression of ATP6V1B1 and associated clinicopathological features have been linked to various cancers; however, its role in epithelial ovarian cancer (EOC) has remained to be explored. The present study aimed to unveil the function, molecular mechanisms and clinical significance of ATP6V1B1 in EOC. The mRNA levels of ATP6V1 subunits A, B1 and B2 in EOC tissues were determined using data from the Gene Expression Profiling Interactive Analysis database and RNA sequencing. Protein levels of ATP6V1B1 were evaluated through immunohistochemistry staining of EOC, borderline, benign and normal epithelial tissues. The association between ATP6V1B1 expression and clinicopathological features and prognosis of patients with EOC was analyzed. Furthermore, the biological role of ATP6V1B1 in ovarian cancer cell lines was also assessed. RNA sequencing and public dataset analyses revealed elevated ATP6V1B1 mRNA levels in EOCs. High ATP6V1B1 protein levels were also observed in EOC compared with those of borderline and benign tumors and nonadjacent normal epithelial tissues. High ATP6V1B1 expression was associated with the serous cell type, advanced International Federation of Gynecology and Obstetrics stage, high/advanced tumor grade, elevated serum cancer antigen 125 levels and platinum resistance (P<0.001, P<0.001, P=0.035, P=0.029 and P=0.011, respectively). High expression levels of ATP6V1B1 were also associated with poor overall and disease-free survival (P<0.001). Knockdown of ATP6V1B1 decreased cancer cell proliferation and colony-forming abilities (P<0.001) *in vitro* by inducing cell cycle arrest in G0/G1 phase. Significant upregulation of ATP6V1B1 was observed in EOC and the prognostic significance and association with chemotherapy resistance of ATP6V1B1 in EOC was demonstrated, rendering it an EOC-related biomarker for prognostic evaluation and chemotherapy resistance, as well as a potential therapeutic target for patients with EOC.

Introduction

Epithelial ovarian cancer (EOC) is one of the most prevalent and fatal malignant diseases of the female genital tract, with an estimated 21,410 new cases and 13,770 cancer-related deaths in the US in 2021 (1,2). Debulking surgery followed by platinum-based adjuvant chemotherapy is the mainstay of EOC management with an effective response rate of >90% in patients with EOC. However, the 5-year survival rate of patients with EOC remains low at ~40% and only a modest improvement has been achieved in the past decade. Of note, the introduction of anticancer therapeutic agents, including antiangiogenic drugs and polyadenosine diphosphate-ribose polymerase inhibitors, has led to a significant improvement in disease-free survival (DFS) for EOC, as demonstrated in the randomized phase III AURELIA (ENGOT-ov3/AGO-OVAR2.15) trial (3-7).

Correspondence to: Professor Hanbyoul Cho, Department of Obstetrics and Gynecology, Yonsei University College of Medicine, 211 Eonju-Ro, Gangnam-Gu, Seoul 06299, Republic of Korea
E-mail: hanbyoul@yuhs.ac

The unfavorable prognosis of EOC is attributed to the lack of effective clinical screening methods in the early stages of the disease, resulting in diagnosis at advanced stages with most patients ultimately acquiring resistance to platinum-based chemotherapy (8). Thus, identifying new biomarkers and therapeutic targets is crucial to effectively diagnose, treat, and predict the progress and outcome of EOC, including the response to chemotherapy.

A sophisticated web of cellular signaling channels is necessary for cells to detect and react to intrinsic, external inputs to keep homeostasis. However, when these pathways are changed, an impact exists on a variety of cellular functions eventually disrupting homeostasis and encouraging carcinogenesis and cancer growth. Ion exchangers, such as the vacuolar-type proton-translocating ATPase (H^+-ATPases), have a critical role in controlling organelle pH and preserving pH equilibrium among the complex dynamic processes that regulate homeostasis (9-12). Various studies have explored the disruption of H+-ATPases, which promote cancer development, advancement and resistance to chemotherapy by causing extracellular acidosis in specific tissues (13-16). It has been indicated that the presence of V-ATPase on the surface of tumor cells encourages vesicular trafficking and activation of proteases, which in turn contributes to malignancy (17). New strategies to selectively inhibit V-ATPase are being explored to suppress tumor growth and invasion in various types of solid carcinoma, such as colorectal cancer, breast cancer and renal cell carcinoma (18-21).

V-ATPases are multisubunit transmembrane protein transporters composed of 13 subunits organized into two major domains, V_1 and V_0 (22,23). Among the two major domains, V_1, also called ATPase H+ transporting V1 (ATP6V1), is composed of subunits A-H. Of these, the A and B subunits form a hexametric barrel and are directly responsible for ATP hydrolysis (23-25). Numerous investigations have revealed that ATP6V is crucial for the development of several disorders, including diabetes, kidney disease, cancer and improper bone growth (11,13,26). However, the connection between ATP6V1 and EOC has remained to be explored. Furthermore, the expression patterns of ATP6V1 isoforms in EOC remain incompletely understood.

The present study aimed to examine the expression patterns of the ATP6V1 isoforms and demonstrate the clinical significance of ATP6V1 subunit B1 (ATP6V1B1) in serous ovarian cancer cell lines using data from RNA sequencing (RNA-seq) and public databases. Furthermore, the clinicopathological characteristics, including anticancer drug resistance and prognostic value of ATP6V1B1 in EOC, were analyzed.

Materials and methods

Patients and tumor specimens. A total of 213 EOCs, 60 borderline tumors, 109 benign tumors and 80 nonadjacent normal epithelial tissues were obtained from patients who underwent primary cytoreductive surgery at the Gangnam Severance Hospital (Seoul, Korea) between 1996 and 2012 and the Korean Gynecologic Cancer Bank as part of the Bio and Medical Technology Development Program of the Ministry of the National Research Foundation of Korea. Written informed consent from each patient was obtained after providing a

detailed explanation of the study procedures and approval was obtained from the Regional Institutional Review Board (IRB) of the Gangnam Severance Hospital (IRB no. 3-2020-0377). For this study, patients with EOC who had undergone maximal debulking surgery and were treated with carboplatin and paclitaxel chemotherapy were included. Patients who had previously received neoadjuvant chemotherapy were excluded. The inclusion criteria were based on the availability of histologically confirmed tumor stage and grade according to the International Federation of Gynecology and Obstetrics (FIGO) and World Health Organization grading systems, respectively. Clinical information, such as age, disease-free survival (DFS), overall survival (OS), survival status, tumor grade, cell type and response to chemotherapy, was retrieved from patients' medical records. The response to chemotherapy was assessed using the Response Evaluation Criteria in Solid Tumors (version 1.1) (27).

Public database. The Gene Expression Profiling Interactive Analysis (GEPIA) database (http://gepia.cancer-pku.cn) was used to assess the mRNA expression levels of ATP6V1 subunits A, B1 and B2 (28). Three publicly available datasets [i.e., GSE6008 (29), GSE14407 (30) and GSE36668 (31)] that analyzed DEGs between normal ovarian epithelial tissues and high-grade serous ovarian cancer (HGSOC) samples were downloaded from the gene expression omnibus (GEO) database (https://www.ncbinlm.nih.gov/geo/) to validate the RNA-seq data generated in the present study. The expression levels of ATP6V1B1 in platinum-sensitive and -resistant EOC tissues were assessed using the GSE15622 dataset (32). The GEO dataset was searched using the following keywords: 'Homo sapiens', 'epithelial ovarian cancer' and 'normal ovarian epithelium', 'platinum sensitive' and 'platinum resistance'. In addition, only publications with available raw microarray gene expression data, clinical treatment and response information and only two microarray platforms, GPL96 (HG-U133A) and GPL570 (HG-U133 Plus 2.0; Affymetrix; Thermo Fisher Scientific, Inc.), were included.

Laser-capture microdissection, RNA extraction and quality control. The desired lesions from the tissues were microdissected using an AS LMD laser microdissection system (Leica Microsystems, Inc.) according to the manufacturer's instructions after all formalin-fixed paraffin-embedded (FFPE) tissue slides stained with hematoxylin and eosin were reviewed by an experienced gynecological pathologist. Sectioned FFPE tissues were placed on a polyethylene terephthalate membrane (Leica Microsystems, Inc.) and total RNA was extracted using TRIzol reagent (Invitrogen; Thermo Fisher Scientific, Inc.). RNA was quantified using a NanoDrop-2000 spectrophotometer (Thermo Fisher Scientific, Inc.). The quality of the extracted RNA was measured using an Agilent 2100 bioanalyzer equipped with an RNA 6,000 Nano Chip (Agilent Technologies, Inc.).

Library preparation, RNA sequencing read mapping and gene expression analysis. Library construction was performed using the QuantSeq 3' mRNA-Seq Library Prep Kit (Lexogen GmbH) according to the manufacturer's instructions for control and test RNAs. In brief, 500 ng of total

RNA was prepared for the control and experimental RNAs. RNA was hybridized with an oligo-dT primer using First Standard cDNA Synthesis Mix included in the QuantSeq 3' mRNA-Seq Library Prep Kit (Lexogen GmbH), including an Illumina-compatible sequence at its 5' end. Reverse transcription (RT) was performed and after the RNA template was degraded using RNA Removal Solution in the Kit (Lexogen GmbH), a random primer with an Illumina-compatible linker sequence at its 5' end was used for second-strand synthesis using Second Strand Synthesis Mix contained in the kit (Lexogen GmbH). The double-stranded library was purified using the Purification Module with Magnetic Beads included in the kit (Lexogen GmbH). Complete adapter sequences using the Lexogen i7 6 nt Index set (Lexogen GmbH) were added to this library to perform cluster generation and PCR components were removed from the final library using the Purification Module with Magnetic Beads included in the kit (Lexogen GmbH). NextSeq 500 (Illumina, Inc.) was used for single-end 75 base pair high-throughput sequencing. The FASTQ raw data for nine independent libraries were obtained through sequencing: Two were normal epithelial tissues and seven were EOC tissues. Among the seven EOC tissues, four were platinum-sensitive and three were platinum-resistant. All FASTQ reads were trimmed for quality control and adapters were trimmed using Bbduk (BBMap v36.59) (33) and FASTQC (v0.11.7) (34) for sequencing data. Read mapping was performed through the STAR-HTSeq workflow, i.e., STAR (v2.7.3a) (35) and HTSeq-count (v0.12.4) (36), where the reference genome (GRCh38) and annotation were aligned with the sequencing reads. Normalization and differential expression analyses on gene expression levels were performed using the DESeq2 v1.26.0 R package (37), where a normalization method was applied as a variance-stabilizing transformation after performing read counts. Differentially expressed genes (DEGs) were obtained based on the two following criteria: i) Adjusted P-value (i.e., Benjamini and Hochberg method) <0.05; and ii) absolute $\log_2$ (fold change) >2.

Tissue microarray (TMA) and immunohistochemistry. A TMA was constructed with tissue cores of 1.0 mm in diameter containing a sufficient proportion of tumor cells punched from the donor FFPE tissues or tissue blocks using a tissue array (Beecher Instruments, Inc.), and TMA blocks were sliced to 5-μm thickness using a rotary microtome. The TMA sections were deparaffinized with xylene after sectioning and rehydrated in serially graded ethanol to distilled water. Antigen retrieval for antiATP6V1B1 (rabbit polyclonal antibody; cat. no. HPA031847; 1:150; Sigma-Aldrich; Merck KGaA) was performed by incubating TMA sections in a steam pressure cooker (Pascal; Dako; Agilent Technologies, Inc.) containing heat-activated antigen retrieval buffer (Dako; Agilent Technologies, Inc.) at pH 6.0 antigen retrieval buffer (Dako; Agilent Technologies, Inc), at 125°C for 2 min is a Pascal pressure cooker (Dako; Agilent Technologies, Inc.) at 20-23 psi. The sections were then treated with a 3% H_2O_2 solution in methanol for 10 min at room temperature to block the remaining endogenous peroxidase activity. The slides were stained with an ATP6V1B1 antibody for 30 min at room temperature after rinsing. Subsequently, the antigen-antibody reactions were visualized using Envision⁺ Dual

Link System-HRP (Dako; Agilent Technologies, Inc.) and DAB⁺ (3,3'-diaminobenzidine; Dako; Agilent Technologies, Inc.) for 10 min at room temperature. The stained sections were counterstained with hematoxylin after dehydration. Slides were then mounted with Faramount aqueous mounting medium (Dako; Agilent Technologies, Inc.). Negative control immunoglobulin G (IgG) was used in place for primary antibody to evaluate nonspecific staining and the TMA included appropriate positive control specimens.

Evaluation of immunohistochemistry staining. Microscopy images of the stained TMA sections (NanoZoomer 2.0 HT; Hamamatsu Photonics K.K.) at 20x objective magnification (0.5-μm resolution) were captured using high-resolution optical imaging. The scanned sections were analyzed using Visiopharm software, version 6.5.0.2303 (Visiopharm A/S). The intensity of the brown staining was rated on a scale of 0 to 3 (0, negative; 1, weak; 2, moderate; and 3, strong) and the percentage of cytoplasm-stained tumor cells (range, 0-100) was obtained using a predefined optimized algorithm. The total histoscore was determined by multiplying the percentage of positively stained cells by the intensity score (score range, 0-300).

Cell culture. The human ovarian cancer cell line A2780 was purchased from the European Collection of Cell Cultures. OVCA429 and OVCA433 cells were obtained from the Saint Vincent Hospital, The Catholic University of Korea, Suwon, Korea (38,39). OVCAR3, SKOV3 and TOV112D cells were purchased from the American Type Culture Collection. Ovarian cancer cells were cultured in Dulbecco's modified Eagle's medium (DMEM) supplemented with 10% fetal bovine serum (FBS) and 1% penicillin/streptomycin. Three previously established immortalized HOSE cell lines (iHOSE1481, -4138 and -8695) (40) were maintained in DMEM supplemented with 10% FBS and 50 μg/ml gentamicin. All cell lines were incubated at 37°C in a humidified incubator with 5% CO_2.

Small interfering RNA (siRNA) transfection. siRNAs targeting ATP6V1B1 and control siRNA were purchased from Bioneer Corporation. The siRNA sequences are provided in Table SI. OVCAR3 and OVCA433 cells grown in six-well plates were transfected with siRNA at a final concentration of 100 pmol per well using Lipofectamine® RNAiMAX Reagent (Invitrogen; Thermo Fisher Scientific, Inc.), according to the manufacturer's instructions. The knockdown of ATP6V1B1 was verified via RT-quantitative (q)PCR after 48 h of transfection and used for downstream functional experiments.

RT-qPCR. Total RNA was isolated using the AccuPrep® Universal RNA Extraction Kit (Bioneer Corporation) and cDNA was synthesized using the AccuPower® RocketScript™ RT PreMix (Bioneer Corporation) according to the manufacturer's protocol. Gene expression levels were analyzed using the target gene-specific primers listed in Table SI, the ABI 7300 Real-Time PCR System (Applied Biosystems; Thermo Fisher Scientific, Inc.) and TOPreal™ qPCR 2X PreMIX (SYBR Green with high ROX; Enzynomics). Data analysis was performed using the relative quantification method ($2^{-\Delta\Delta Cq}$) to estimate the relative fold changes. All data were

normalized to the GAPDH expression levels. Each experiment was performed in triplicate and with at least three independent replicates.

Cell proliferation assay. Cell proliferation assay was measured using the EZ-Cytox assay kit (Daeil Lab Service) and EdU Cell Proliferation Assay kit (Thermo Fisher Scientific, Inc.) in accordance with the manufacturer's instructions. Concisely, 5×10^3 cells were seeded in 96-well plates after 24 h of transfection. EZ-Cytox reagent was added and the cells were incubated for another 2 h at 37°C. The absorbance at 450 nm was then detected using a microplate reader (Bio-Rad Laboratories, Inc.). The EdU incorporation experiment was also performed according to the user manual. Fluorescence was measured using a FLUOstar Omega instrument (BMG Labtech GmbH) with 568 nm of excitation and 585 nm of emission. Each experiment was performed thrice.

Colony-formation assay. The transfected cells (500 cells/well) were seeded in a six-well plate and incubated at 37°C with 5% CO_2 for 2 weeks. The cells were fixed with methanol for 10 min and stained with 0.5% crystal violet for 30 min at room temperature. Colonies were counted under a microscope after being rinsed with distilled water, and each colony contained at least 50 cells. Each experiment was repeated thrice.

Cell-cycle analysis by flow cytometry. Transfected OVCAR3 and OVCA433 cells were harvested and fixed in 70% ethanol at 4°C. The fixed cells were stained with propidium iodide supplemented with RNAase A (Sigma-Aldrich; Merck KGaA) in the dark at room temperature for 30 min. The relative amount of cells in each phase of the cell cycle was analyzed by flow cytometry (FACSCanto II; BD Biosciences) and evaluated using the FlowJo software _v10.8.0 (FlowJo LLC).

Western blot analysis. Cells were harvested and lysed using a cell lysis buffer (Cell Signaling Technology, Inc.) containing phenylmethylsulfonyl fluoride. Proteins from cell lysates were electrophoresed on a 10-12% SDS-PAGE gel and transferred to a nitrocellulose membrane (Pall Corporation). The membranes were incubated overnight at 4°C with the corresponding primary antibodies of Cyclin D1 (1:1,000; cat. no. 2922; Cell Signaling Technology, Inc.), p21 (1:1,000; cat. no. 2947; Cell Signaling Technology, Inc.) and α-actinin (1:5,000; cat. no. sc-17829; Santa Cruz Biotechnology, Inc.). HRP-conjugated secondary antibodies (1:2,000; cat nos. 7074 and 7076; Cell Signaling Technology, Inc.) were then applied. Immunoreactive bands were visualized using enhanced chemiluminescence reagents (Thermo Fisher Scientific, Inc.).

Statistical analysis. Statistical analysis was performed using either the R statistical package (version 4.2.0) or SPSS version 25.0 (SPSS, Inc.). The expression levels of α-actinin, ATP6V1B and clinicopathological characteristics of EOC when appropriate were assessed using the Mann-Whitney U or Kruskal-Wallis test. The OS and DFS curves were analyzed using the Kaplan-Meier method by grouping the subjects into ATP6V1B1 high- or low-expression groups based on the optimal cut-off point calculated by the 'MaxStat' package of the R software (41). A Cox proportional hazards model was

created to identify independent predictors of survival. $P<0.05$ was considered to indicate statistical significance.

Results

Upregulated expression of ATP6V1B1 in EOC and platinum-resistant EOC. The A and B subunits of ATP6V1 are structurally similar; however, these subunits were reported to have different activity profiles (42). Therefore, data from the GEPIA database were retrieved to evaluate the specific subunit that is upregulated in EOC. ATP6V1B1 was more specifically expressed, among the expressions of three subunits, ATP6V1A, ATP6V1B1 and ATP6V1B2, in EOC than in other cancers (Fig. 1A). DEGs between the normal ovarian epithelial and HGSOC tissues were identified by an Illumina microarray through RNA-seq analysis. RNA isolated from the tissues was directly compared using hybridization with cDNA microarrays containing 24,957 probe sets. The volcano plot indicated 24,958 DEGs ($P<0.05$, fold change >2) in EOC compared with normal epithelial tissues, and one of the DEGs was ATP6V1B1 (Fig. 1B).

The expression of ATP6V1B1 was first examined in three iHOSE cell lines and six ovarian cancer cell lines (i.e., A2780, OVCA429, OVCA433, OBCAR3, SKOV3 and TOV112D) using RT-qPCR to elucidate the molecular mechanisms of ATP6V1B1 in promoting ovarian cancer development. The results indicated that ATP6V1B1 was highly expressed in ovarian cancer cells and lowly expressed in iHOSE cells (Fig. 1C), which was similar to the results obtained from publicly available datasets (GSE6008, GSE14407 and GSE36668) (Fig. 1D). Anticancer therapy resistance may be induced by changes in the normal pH gradient across the plasma membrane, which is influenced by the activity of V-ATPase. The EOC tissues were divided into platinum-sensitive and -resistant groups and the gene expression of ATP6V1B1 was compared between these two groups. ATP6V1B1 was significantly upregulated in platinum-resistant EOCs, as expected. Similar results were observed using data from GSE15622, which compared 42 platinum-sensitive and 26 platinum-resistant EOC tissue samples (Fig. 1E and F). Overall, these observations suggest that the expression of ATP6V1B1 is upregulated in EOC and platinum-resistant EOCs.

Clinicopathological characteristics associated with ATP6V1B1 protein expression in patients with EOC. Next, the protein levels of ATP6V1B1 were compared among nonadjacent normal epithelial tissues, benign and borderline tumors and EOC tissues obtained from 1996 to 2012 using IHC. The average age of patients with EOC included in this study was 52.13±13.08 years. For borderline patients, the average age was 43.23±17.44 years, while for benign patients, it was 43.66±13.89 years (Table SII). The average age of the donors of nonadjacent normal epithelial tissues was 49.12±16.45 years. ATP6V1B1 protein levels gradually increased from normal tissues to EOCs. Representative IHC images are provided in Fig. 2A. ATP6V1B1 protein expression was strongly associated with adverse clinicopathological features of EOC, including advanced FIGO stage ($P<0.001$), serous cell type ($P<0.001$), high tumor grade ($P=0.035$), elevated serum cancer antigen (CA)-125 levels ($P=0.029$ and platinum resistance ($P=0.011$) (Table I).
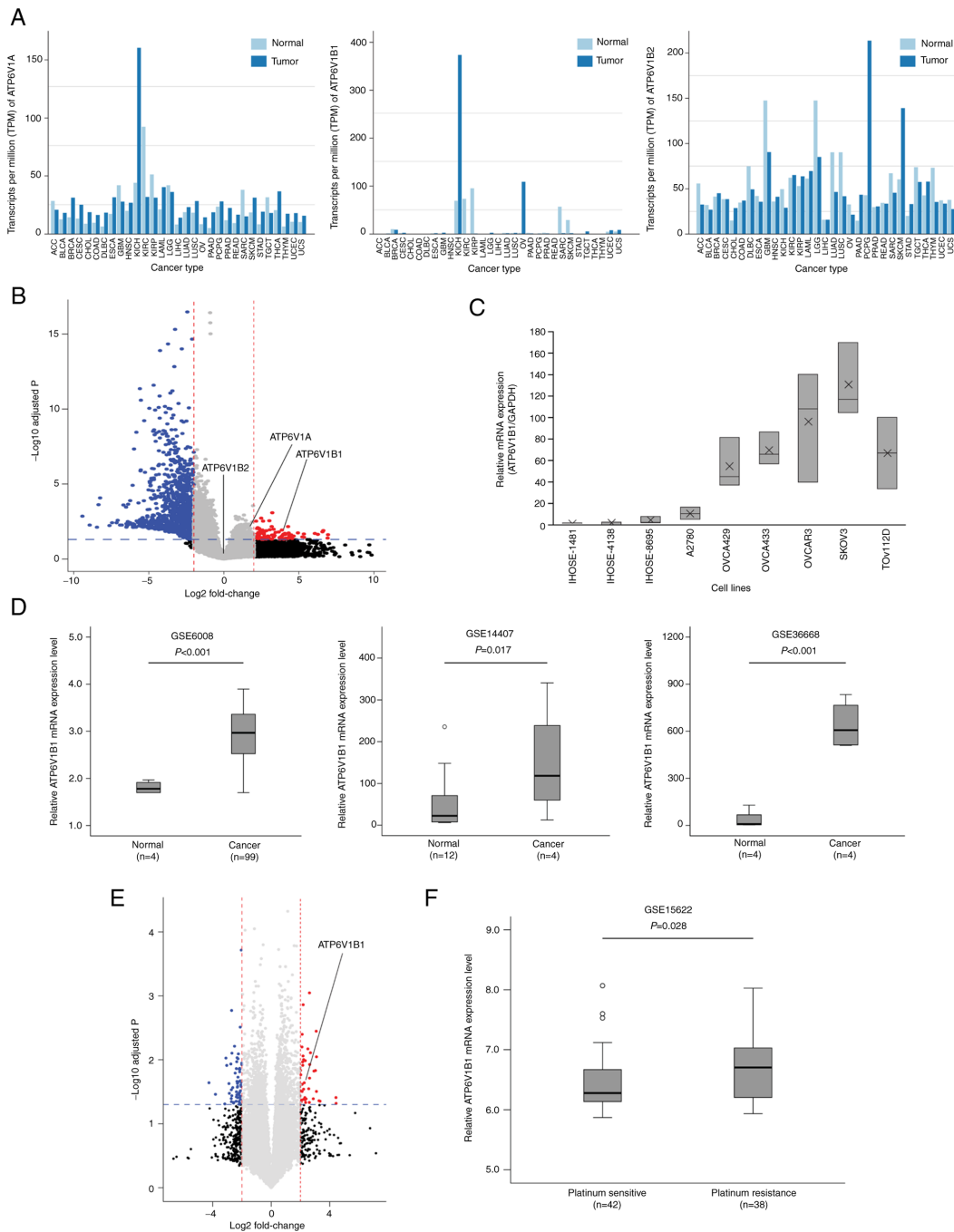
Figure 1. Comparative analysis of ATP6V1 expression in EOC. (A) Gene Expression Profiling Interactive Analysis was performed to validate the expression of ATP6V1 subunits A, B1 and B2 in various cancers. (B) Volcano plot of the distribution of differentially expressed genes between normal ovarian epithelial tissues and EOC tissues in an RNA sequencing analysis (P<0.05 and fold change >2) demonstrating the upregulation of ATP6V1A, ATP6V1B1 and ATP6V1B2 expression in EOCs. The -$\log_{10}$ (P-value) of each gene is plotted against the $\log_2$ ratio of cancer to normal intensity. Vertical dotted lines in red and blue correspond to a 2.0-fold upregulation and downregulation of expression, respectively. Horizontal blue dotted lines indicate the significance level at P=0.05. Plots were generated using ExDEGA v.1.6.5 software. (C) mRNA expression of ATP6V1B1 in immortalized human ovarian epithelial cell lines (iHOSE 1481, iHOSE 4138, and iHOSE 8695) and six ovarian cancer cell lines determined using reverse transcription-quantitative PCR. The expression levels of ATP6V1B1 were normalized to GAPDH expression levels. (D) Box plots of the mRNA expression of ATP6V1B1 between normal and high-grade serous ovarian cancer samples. Publicly available gene expression data were obtained from the GEO database (i.e., GSE6008, GSE14407 and GSE36668). (E) Volcano plot of the distribution of differentially expressed genes between platinum-sensitive and -resistant EOC tissues in the RNA sequencing analysis (P<0.05 and fold change >2). Vertical dotted lines in red and blue correspond to a 2.0-fold upregulation and downregulation of expression, respectively. Horizontal blue dotted lines indicate the significance level at P=0.05. (F) Publicly available relative ATP6 V1B1 mRNA expression data between platinum-sensitive and -resistant EOC tissues were obtained from the GEO database (i.e., GSE15622). ACC, adrenocortical carcinoma; ATP6V1B1, ATPase H+ transporting V1 subunit B1; BLC, bladder urothelial carcinoma; BRCA, breast invasive carcinoma; CESC, cervical squamous cell carcinoma and endocervical adenocarcinoma; CHOL, cholangiocarcinoma; COAD, colon adenocarcinoma; DLBC, lymphoid neoplasm diffuse large B-cell lymphoma; EOC, epithelial ovarian cancer; ESCA, esophageal carcinoma; GBM, glioblastoma multiforme; GEO, Gene Expression Omnibus; HNSC, head and neck squamous cell carcinoma; KICH, kidney chromophobe; KIRC, kidney renal clear cell carcinoma; KIRP, kidney renal papillary cell carcinoma; LAML, acute myeloid leukemia; LGG, brain lower-grade glioma; LIHC, liver hepatocellular carcinoma; LUAD, lung adenocarcinoma; LUSC, lung squamous cell carcinoma; OV, ovarian serous cystadenocarcinoma; PAAD, pancreatic adenocarcinoma; PCPG, pheochromocytoma and paraganglioma; PRAD, prostate adenocarcinoma; READ, rectum adenocarcinoma; SARC, sarcoma; SKCM, skin cutaneous melanoma; STAD, stomach adenocarcinoma; TGCT, testicular germ cell tumors; THCA, thyroid carcinoma; THYM, thymoma; UCEC, uterine corpus endometrial carcinoma; UCS, uterine carcinosarcoma; TPM, transcripts per million.
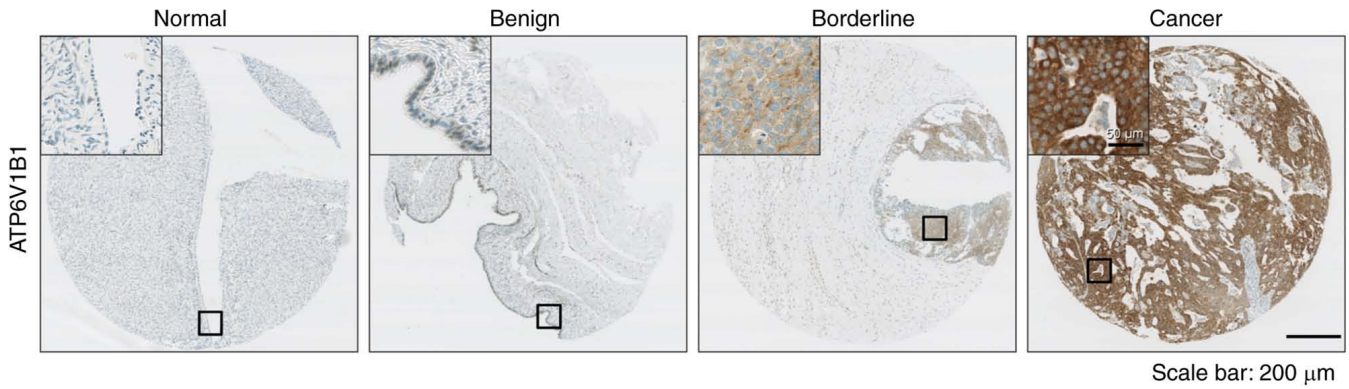
Figure 2. Representative immunohistochemical staining images of ATP6V1B1 in nonadjacent ovarian epithelial tissues (normal), benign and borderline tumor and epithelial ovarian cancer (scale bar; 200 and 50 μm in the magnified windows).

Relationship between ATP6V1B1 expression and prognosis in patients with EOC. The prognostic significance of ATP6V1B1 expression in patients with EOC was then evaluated using Kaplan-Meier analysis. High ATP6V1B1 expression was significantly associated with poor DFS and OS (both P<0.001; Fig. 3A). In addition, FIGO stage III/IV was significantly associated with poor DFS and OS, which was expected and further validated in the present analysis (Fig. 3B). The multivariate Cox analysis suggested that high ATP6V1B1 expression was an independent prognostic factor for both DFS [hazard ratio (HR)=2.10 (95% CI, 1.23-3.58), P=0.006] and OS [HR=2.57 (95% CI, 1.12-5.94), P=0.027] (Table II). In summary, the results of the present study demonstrated that high ATP6V1B1 expression may be a predictive biomarker for poor prognosis in patients with EOC.

Knockdown of ATP6V1B1 expression inhibits ovarian cancer cell proliferation. ATP6V1B1 was silenced using siRNA targeting ATP6V1B1 in OVCAR3 and OVCA433 cells to assess the biological consequences of ATP6V1B1 overexpression in ovarian cancer cells. The knockdown of ATP6V1B1 was verified using RT-qPCR (Fig. 4A). Further examination of cell proliferation using EZ-Cytox (Fig. 4B) and EdU incorporation assays (Fig. 4C) indicated that ATP6V1B1 knockdown significantly inhibited cell proliferation in both OVCAR3 and OVCA433 cells. Similarly, knockdown of ATP6V1B1 decreased the number of colonies formed (Fig. 4D).

Knockdown of ATP6V1B1 induces G0/G1-phase cell cycle arrest in ovarian cancer cells. A previous study indicated that V-ATPase inhibition neutralizes lysosomal pH and induces cell cycle arrest and apoptosis in various epithelial cells (43). In the present study, cell cycle progression was analyzed to examine the underlying mechanisms of the antiproliferative effects observed in cells transfected with siRNA targeting ATP6V1B1. Flow cytometric analysis of the cell cycle distribution revealed that knockdown of ATP6V1B1 resulted in a significant increase in the number of cells in the G0/G1-phase compared with that of the control (Fig. 5A and B). The mRNA and protein expression levels of cell cycle regulation proteins cyclin D1 and p21, which promote G1/S transition, were assessed to elucidate the mechanism by which ATP6V1B1 knockdown blocks G1 progression. Both the mRNA and

protein expression results revealed upregulation of p21 and downregulation of cyclin D1 in ATP6V1B1 knockdown cells (Fig. 5C and D).

Discussion

Proton pumps, such V-ATPases, have increased activity in tumor cells and contribute to the maintenance of an acidic extracellular microenvironment and intracytoplasmic alkalization, which eventually fosters medication tolerance and tumor metastasis (44,45). Various studies have focused on investigating the oncogenic role of V-ATPases, which are among the most well-known proton pumps that are composed of eight subunits, and demonstrated that their expression is positively associated with cancer invasion and metastasis (46,47). Furthermore, studies examining specific V-ATPases isoforms have been conducted. ATP6V1C1 is overexpressed in breast cancer and Barrett's esophagus, which is a precursor lesion of esophageal squamous cell carcinoma, and its overexpression is associated with poor outcomes (48-50). The expression of V-ATPase-specific subunits has also been examined in pancreatic cancer (51,52), non-small cell lung cancer (53), oral squamous cell carcinoma (54,55), EOC (56) and cervical cancer (57), further indicating the roles of V-ATPase subunits in carcinogenesis. However, to the best of our knowledge, the association between the expression of V-ATPase isoforms and cancer progression has remained elusive. In the present study, the expression of V-ATPase V1 subunits A and B, which are components of the central stator of the proton pump, was examined in EOC.

Subunits V1A and V1B mediate ATP hydrolysis at the three reaction sites and increasing evidence suggests that these subunits are likely to have functional consequences for the entire pump (42). Therefore, in the present study, the expression levels of subunits V1A, V1B1 and V1B2 were analyzed using data from RNA-seq and public databases. Furthermore, the clinical significance of the upregulation of ATP6V1B1 in EOC was explored. The IHC results indicated a gradual increase in protein expression of ATP6V1B1 from normal ovarian epithelial tissues to benign and borderline tumors to EOCs. Elevated ATP6V1B1 expression was highly associated with advanced FIGO stage, serous cell type, poor tumor grade and elevated CA-125 levels, indicating that ATP6V1B1 may be

Table I. Association between clinicopathologic features and ATPase H+ transporting V1 subunit B1 expression in patients with epithelial ovarian cancer.

Item	N (%)	Mean score of ATP6V1B1 IHC (95% CI)	P-value
Diagnostic category			<0.001
Normal	72 (18.8)	9.00 (6.12-11.88)	
Benign	91 (23.8)	29.48 (20.38-38.59)	
Borderline	48 (12.6)	67.67 (50.88-84.46)	
Cancer	171 (44.8)	105.52 (92.56-118.49)	
FIGO stage			0.001
I-II	57 (33.3)	74.59 (54.02-95.16)	
III-IV	114 (66.7)	121.51 (101.46-137.56)	
Cell type			<0.001
Serous	113 (66.1)	129.46 (113.77-154.04)	
Others	28 (16.4)	58.49 (40.45-46.52)	
N/A	30 (17.5)		
Tumor grade			0.035
Low/moderate	79 (46.2)	91.54 (73.74-109.34)	
High	82 (48.0)	120.85 (100.18-141.51)	
N/A	10 (5.8)		
CA125			0.029
Negative	28 (16.4)	72.76 (44.63-100.90)	
Positive	141 (82.5)	111.84 (97.20-126.47)	
N/A	2 (1.1)		
Chemosensitivity			0.011
Sensitive	144 (84.2)	104.25 (90.34-118.15)	
Resistant	12 (7.0)	169.96 (111.43-228.49)	
N/A	15 (8.8)		

FIGO, International Federation of Gynecology and Obstetrics; CA, cancer antigen; CI, confidence interval; N/A, not available; ATP6V1B1, ATPase H+ transporting V1 subunit B1; IHC immunohistochemistry.

involved in EOC progression. Furthermore, the multivariate analysis indicated that upregulated ATP6V1B1 was an independent prognostic factor for both DFS and OS. Overall, these results suggest that ATP6V1B1 has an important role in the pathogenesis of EOC.

The strength of the present study may have been compromised by the small sample size and inclusion of several histological subtypes. Therefore, future research should include more distinct histological subgroups.

Of note, the knockdown of ATP6V1B1 in EOC decreased proliferation and colony formation but induced cell cycle arrest through the G1 phase, signifying cell cycle arrest at the G0/G1 phase. The present results indicate that the decreases in the number of viable cells and colony-formation abilities were not due to an increase in cell death; however, they may be related to cell proliferation. It may be concluded that knockdown of ATP6V1B1 suppresses tumor cell growth, at least in part, by causing G0/G1-phase cell-cycle arrest via the downregulation of cyclin D and upregulating p21 based on these results. In agreement with the present study, Lim et al (58) reported that the inhibition of V-ATPase by bafilomycin A1 causes apoptosis by inducing cell cycle arrest at the G0/G1 phase and upregulating p21 in prostate, kidney, cervical and liver cancers in vitro and in vivo. Furthermore, the present results support the findings from a previous study reporting that the cell cycle is regulated by both signaling pathways and changes in pH during the cell cycle (59). However, additional studies are required to determine the underlying mechanism, and it may be suggested that the Warburg effect may have a role (60). A previous study reported that elevation of intracellular pH promotes cancer cell proliferation, which, coupled with increased glycolysis and adaptation to hypoxia (i.e., the Warburg effect), upregulates hypoxia-inducible factor-α (HIF-α) (61). The activation of HIF-α increases iron uptake in tumors by inducing transferrin receptor-1 expression or degrading heme into iron, carbon monoxide and biliverdin through the enzyme heme oxygenase. Cancer cells use the BMP-SMAD and JAK-STAT3 pathways to boost the function of hepcidin, a modulation of iron metabolism (62). The expression of cell cycle regulators, such as p21, is altered by higher iron levels, which inhibit prostate cancer growth in the G0/G1 phase (62). Increased iron levels were found to alter the expression of cell cycle regulators, such as p21, which halt prostate cancer growth in the G0/G1 phase (63). A study conducted in 2014 reported that migrating cancer cells are predominantly in the G0/G1 phase, which confer chemoresistance in cancers (64).

Table II. Univariate and multivariate analyses of DFS or OS in patients with epithelial ovarian cancer.

Factor	DFS HR (95% CI), P-value		OS HR (95% CI), P-value	
	Univariate	Multivariate	Univariate	Multivariate
Age (>50 years)	1.58 (1.06-2.35), 0.024	1.02 (0.66-1,60), 0.916	2.12 (1.17-3.84), 0.013	1.48 (0.78-2.81), 0.233
FIGO stage (III-IV)	6.42 (3.33-12.39), <0.001	3.78 (1.82-7.86), <0.001	5.10 (2.02-12.86), 0.001	2.90 (1.12-7.53), 0.029
Cell type (serous)	0.33 (0.20-0.55), <0.001	0.60 (0.32-1.13), 0.113	0.22 (0.09-0.56), 0.001	0.39 (0.13-1.12), 0.080
Tumor grade (poor)	1.95 (1.28-2.97), 0.002	1.63 (1.04-2.54), 0.032	1.69 (0.95-3.00), 0.076	NA
CA125[+] (>35 U/ml)	2.39 (1.20-4.74), 0.013	1.05 (0.48-2.27), 0.907	2.22 (0.80-6.16), 0.127	NA
ATP6V1B1+[a]	3.47 (2.10-5.74), <0.001	2.10 (1.23-3.58), 0.006	4.42 (1.96-9.94), <0.001	2.57 (1.12-5.94), 0.027

[a]Cut-off value of ATP6V1B1[+] was an immunohistochemistry score >76.35. OS, overall survival; DFS, disease-free survival; HR, hazard ratio; CI, confidence interval; CA, cancer antigen; FIGO, International Federation of Gynecology and Obstetrics; ATP6V1B1, ATPase H+ transporting V1 subunit B1.
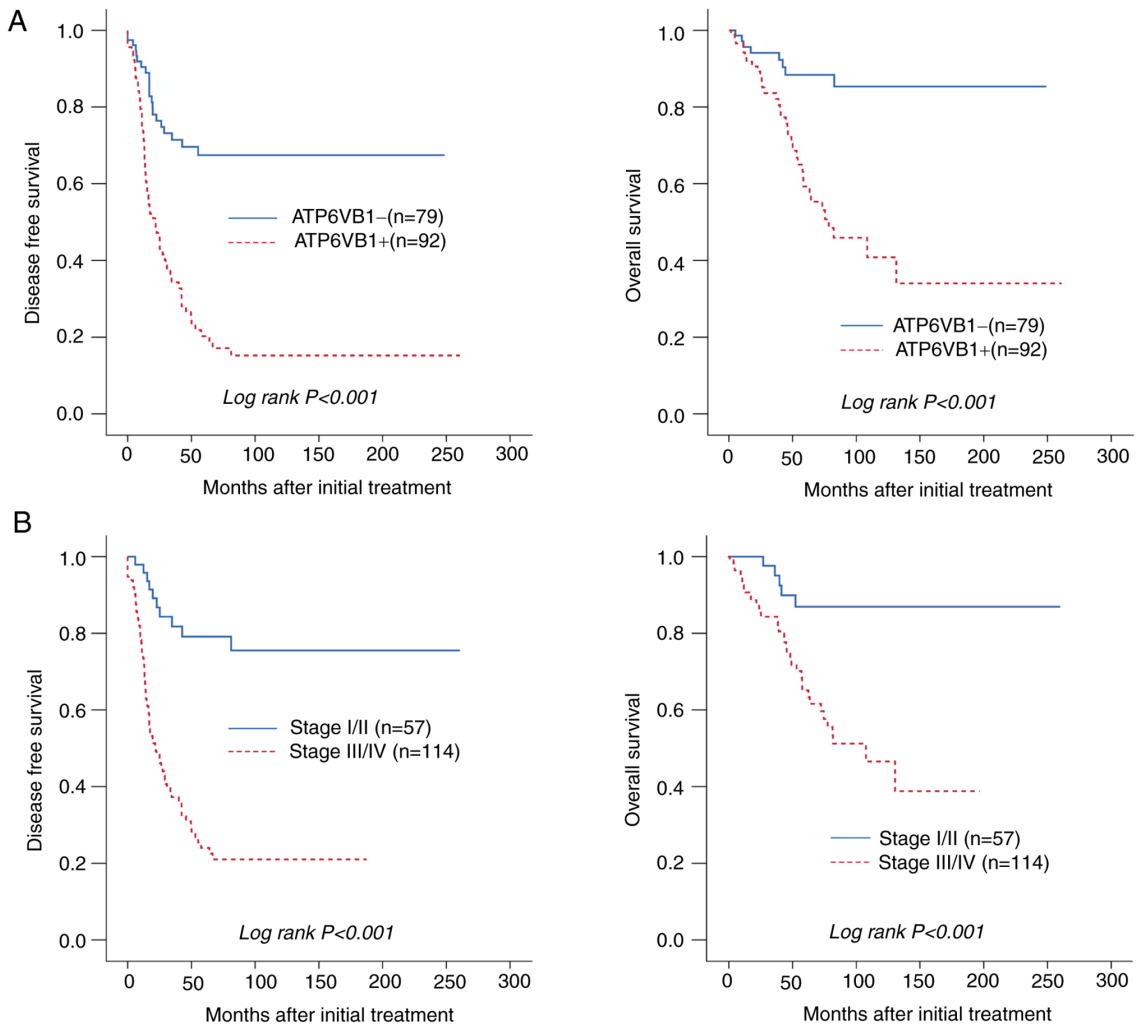
Figure 3. Kaplan-Meier survival curve of ATP6V1B1 expression in patients with EOC. (A) Disease-free and overall survival of patients with EOC analyzed according to ATP6V1B1 expression. (B) Disease-free and overall survival of patients with EOC according to the International Federation of Gynecology and Obstetrics stage. ATP6V1B1, ATPase H+ transporting V1 subunit B1; EOC, epithelial ovarian cancer.
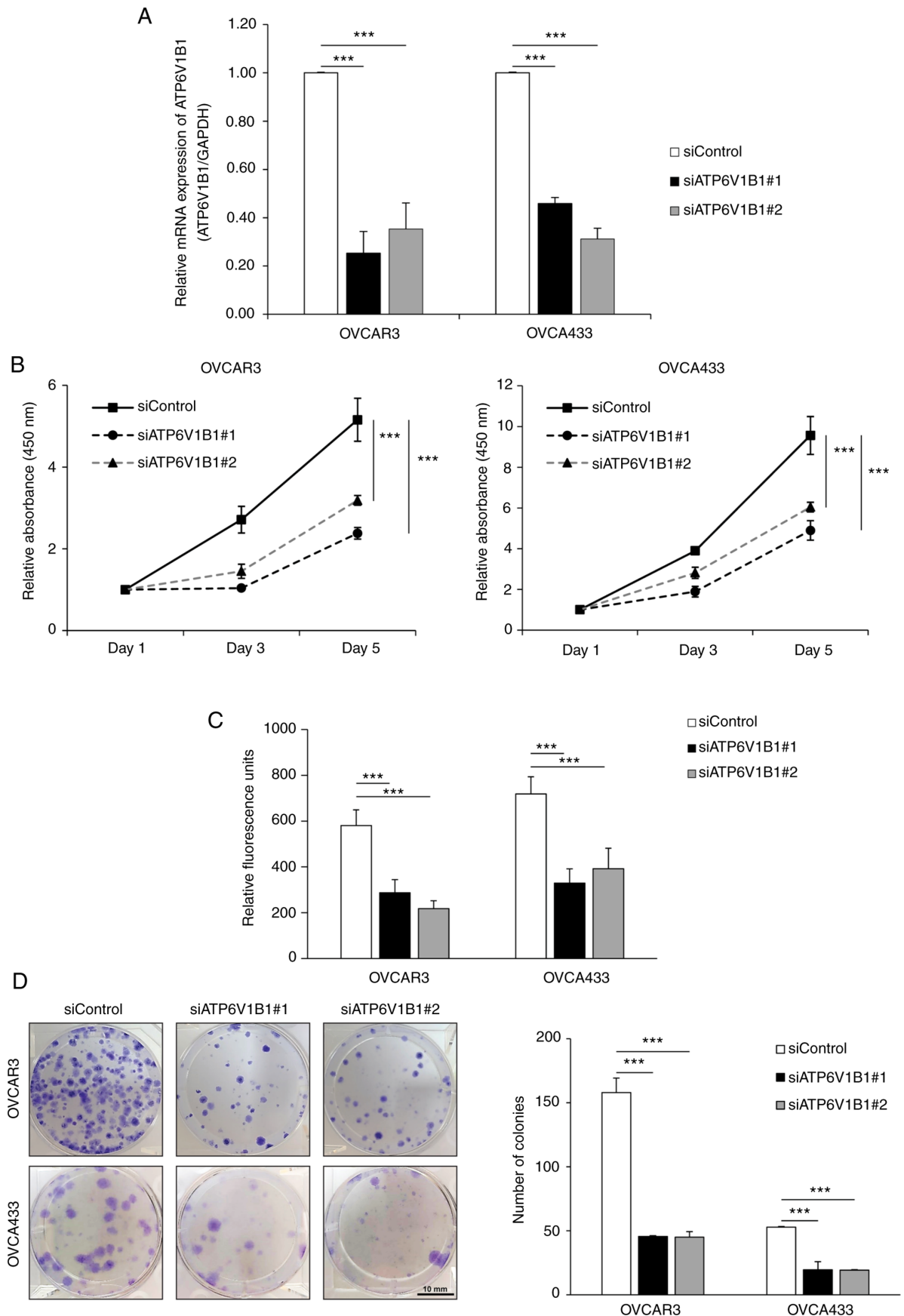
Figure 4. Knockdown of ATP6V1B1 expression inhibits ovarian cancer cell proliferation. (A) OVCAR3 and OVCA433 cells were transfected with siRNA against ATP6V1B1 for 48 h. The knockdown of ATP6V1B1 was verified using reverse transcription-quantitative PCR. (B and C) The proliferation of siRNA-NC and siRNA-ATP6V1B1 cells was detected using the (B) EZ-Cytox and (C) EdU incorporation assays. (D) A colony-formation assay was performed using siRNA-NC- and siRNA-ATP6V1B1-transfected cells. Left panel: Representative image of the colony-formation assay (scale bar, 10 mm). Right panel: Quantitative results of the colony-formation assay. Values are expressed as the mean ± standard error of triplicate experiments. ***P<0.001. NC, negative control; siRNA, small interfering RNA; ATP6V1B1, ATPase H+ transporting V1 subunit B1.
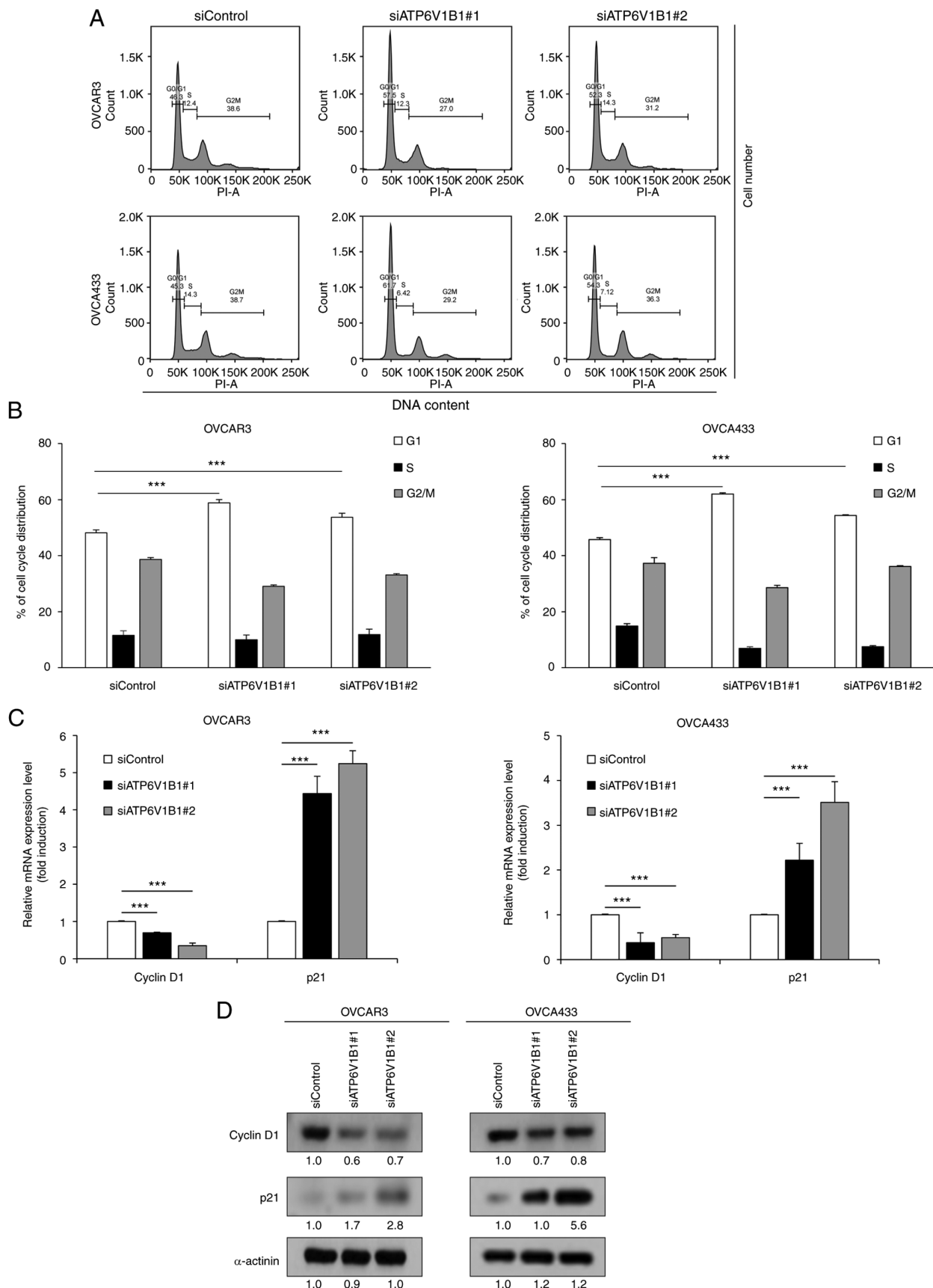
Figure 5. Knockdown of ATP6V1B1 expression induces cell-cycle arrest of ovarian cancer cells in G0/G1-phase. (A) Cell-cycle distributions of siRNA-NC and siRNA-ATP6V1B1-transfected cells were analyzed using flow cytometry after propidium iodide staining. The percentage of cells in the G0/G1, S and G2/M phases was calculated using the FlowJo software. (B) The percentages of cells in the different phases of the cell cycle from A are presented in a bar chart. (C) The mRNA expression levels of cyclin D1 and p21 were analyzed using reverse transcription-quantitative PCR. The expression levels were normalized to GAPDH expression levels. (D) The protein levels of cyclin D1, p21 and α-actinin were determined by western blot analysis. The numbers below each blot represent densitometric values. Values are expressed as the mean ± standard error of triplicate experiments. ***P<0.001. NC, negative control; siRNA, small interfering RNA; ATP6V1B1, ATPase H+ transporting V1 subunit B1.

The clinicopathological characteristics of EOC specimens and RNA-seq data revealed that ATP6V1B1 overexpression is associated with platinum-based chemotherapy resistance. Studies relating chemotherapy resistance in cancer cells to the reversal of the typical pH gradient between the cytoplasm and extracellular environment, which controls the G0/G1 phase of the cell cycle, may help to partially explain this. Overall, therapeutic strategies to maintain the pH gradient across the plasma membrane appear to be effective in enhancing the effectiveness of platinum-based chemotherapy (13).

In the present study, the clinical and prognostic significances of ATP6V1B1 were demonstrated. ATP6V1B1 protein expression was the lowest in the nonadjacent normal ovarian epithelial tissues and its expression gradually increased from benign to borderline tumors and was expressed the highest in the EOC tissues. Overexpression of ATP6V1B1 was positively correlated with adverse clinicopathological parameters and has an independent prognostic value for DFS and OS, further supporting its use as a valuable biomarker for treatment response and prognosis for EOC. Of note, including ATP6V1B1 in the subset of gene panels would be more effective to facilitate a personalized therapy and increase the survival of patients with EOC as new avenues of EOC molecular characterization were opened using next-generation/high-throughput sequencing technology to predict platinum resistance or prognosis (65,66). In addition, the present study suggested that ATP6V1B1 may have a mechanistic role in enhancing cell motility via the disruption of the cell cycle, making it a viable therapeutic target.

Availability of data and materials

The datasets generated and/or analyzed during the current study are available from the Sequence Read Archive repository with the accession no. PRJNA929551 (https://dataview.ncbi.nlm.nih.gov/object/PRJNA929551?reviewer=2a8ackbu9q2e6l33nhhh8aonfq).

Authors' contributions

Conceptualization, HY, GHH, JYC and HC; methodology, GHH, JHK, JYC and HC; data curation, GHH, HY and HC; investigation, HY; writing-original draft preparation, HY and GHH; and writing-review and editing, JYC, JHK and HC. GHH, HY and HC confirmed the authenticity of all the raw data. All authors have read and approved the final manuscript.

Ethics approval and consent to participate

All biological samples were collected after obtaining informed consent from the participants following the guidelines of the IRB of Gangnam Severance Hospital, and the present study was approved by the IRB of Gangnam Severance Hospital (Seoul, Korea; IRB no. 3-2020-0377).

Patient consent for publication

Not applicable.

Competing interests

The authors declare that they have no competing interests.

References

1. Sung H, Ferlay J, Siegel RL, Laversanne M, Soerjomataram I, Jemal A and Bray F: Global cancer statistics 2020: GLOBOCAN estimates of incidence and mortality worldwide for 36 cancers in 185 countries. CA Cancer J Clin 71: 209-249, 2021.
2. Siegel RL, Miller KD, Fuchs HE and Jemal A: Cancer statistics, 2021. CA Cancer J Clin 71: 7-33, 2021.
3. Siegel RL, Miller KD and Jemal A: Cancer statistics, 2020. CA Cancer J Clin 70: 7-30, 2020.
4. Lheureux S, Gourley C, Vergote I and Oza AM: Epithelial ovarian cancer. Lancet 393: 1240-1253, 2019.
5. Perren TJ, Swart AM, Pfisterer J, Ledermann JA, Pujade-Lauraine E, Kristensen G, Carey MS, Beale P, Cervantes A, Kurzeder C, et al: A phase 3 trial of bevacizumab in ovarian cancer. N Engl J Med 365: 2484-2496, 2011.
6. Pujade-Lauraine E, Ledermann JA, Selle F, Gebski V, Penson RT, Oza AM, Korach J, Huzarski T, Poveda A, Pignata S, et al: Olaparib tablets as maintenance therapy in patients with platinum-sensitive, relapsed ovarian cancer and a BRCA1/2 mutation (SOLO2/ENGOT-Ov21): A double-blind, randomised, placebo-controlled, phase 3 trial. Lancet Oncol 18: 1274-1284, 2017.
7. Pujade-Lauraine E, Hilpert F, Weber B, Reuss A, Poveda A, Kristensen G, Sorio R, Vegote I, Witteveen P, Bamias A, et al: Bevacizumab combined with chemotherapy for platinum-resistant recurrent ovarian cancer: The AURELIA open-label randomized phase III trial. J Clin Oncol 32: 1302-1308, 2014.
8. Bast RC Jr, Hennessy B and Mills GB: The biology of ovarian cancer: New opportunities for translation. Nat Rev Cancer 9: 415-428, 2009.
9. Nishi T and Forgac M: The vacuolar (H+)-ATPases-nature's most versatile proton pumps. Nat Rev Mol Cell Biol 3: 94-103, 2002.
10. Forgac M: Vacuolar ATPases: Rotary proton pumps in physiology and pathophysiology. Nat Rev Mol Cell Biol 8: 917-929, 2007.
11. Marshansky V, Rubinstein JL and Grüber G: Eukaryotic V-ATPase: Novel structural findings and functional insights. Biochim Biophys Acta 1837: 857-879, 2014.
12. Toyomura T, Oka T, Yamaguchi C, Wada Y and Futai M: Three subunit a isoforms of mouse vacuolar H+-ATPase: Preferential expression of the a3 isoform during osteoclast differentiation. J Biol Chem 275: 8760-8765, 2000.
13. Stransky L, Cotter K and Forgac M: The function of V-ATPases in cancer. Physiol Rev 96: 1071-1091, 2016.
14. Morita T, Nagaki T, Fukuda I and Okumura K: Clastogenicity of low pH to various cultured mammalian cells. Mutat Res 268: 297-305, 1992.
15. Martínez-Zaguilán R, Seftor EA, Seftor RE, Chu YW, Gillies RJ and Hendrix MJ: Acidic pH enhances the invasive behavior of human melanoma cells. Clin Exp Metastasis 14: 176-186, 1996.

16. Fais S, De Milito A, You H and Qin W: Targeting vacuolar H+-ATPases as a new strategy against cancer. Cancer Res 67: 10627-1030, 2007.

17. Holliday LS: Vacuolar H+-ATPase: An essential multitasking enzyme in physiology and pathophysiology. New J Sci 2014: 1-21, 2014.

18. Zhang F, Shen H, Fu Y, Yu G, Cao F, Chang W and Xie Z: Vacuolar membrane ATPase activity 21 predicts a favorable outcome and acts as a suppressor in colorectal cancer. Front Oncol 10: 605801, 2020.

19. Nishie M, Suzuki E, Hattori M, Kawaguch K, Kataoka TR, Hirata M, Pu F, Kotake T, Tsuda M, Yamaguchi A, *et al*: Downregulated ATP6V1B1 expression acidifies the intracellular environment of cancer cells leading to resistance to antibody-dependent cellular cytotoxicity. Cancer Immunol Immunother 70: 817-830, 2021.

20. Whitton B, Okamoto H, Rose-Zerilli M, Packham G and Crabb SJ: V-ATPase Inhibition decreases mutant androgen receptor activity in castrate-resistant prostate cancer. Mol Cancer Ther 20: 739-748, 2021.

21. Ibrahim SA, Kulshrestha A, Katara GK, Riehl V, Sahoo M and Beaman KD: Cancer-associated V-ATPase induces delayed apoptosis of protumorigenic neutrophils. Mol Oncol 14: 590-610, 2020.

22. Forgac M: Structure, mechanism and regulation of the clathrin-coated vesicle and yeast vacuolar H (+)-ATPases. J Exp Biol 203: 71-80, 2000.

23. Forgac M: Structure and properties of the vacuolar (H+)-ATPases. J Biol Chem 274: 12951-1294, 1999.

24. Bar-Peled L, Schweitzer LD, Zoncu R and Sabatini DM: Ragulator is a GEF for the rag GTPases that signal amino acid levels to mTORC1. Cell 150: 1196-1208, 2012.

25. Vasilyeva E, Liu Q, MacLeod KJ, Baleja JD and Forgac M: Cysteine scanning mutagenesis of the noncatalytic nucleotide binding site of the yeast V-ATPase. J Biol Chem 275: 255-260, 2000.

26. Lozupone F, Borghi M, Marzoli F, Azzarito T, Matarrese P, Iessi E, Venturi G, Meschini S, Canitano A, Bona R, *et al*: TM9SF4 is a novel V-ATPase-interacting protein that modulates tumor pH alterations associated with drug resistance and invasiveness of colon cancer cells. Oncogene 34: 5163-5174, 2015.

27. Kalidos K, Avinash S, Prahladan A, Koshy S and Ramachandran K: Response evaluation criteria in solid tumors (RECIST) version 1.1 in lung cancer: comparison with RECIST version 1.0-a retrospective study 2016: European Society of Radiology (ECR), 2016.

28. Tang Z, Li C, Kang B, Gao G, Li C and Zhang Z: GEPIA: A web server for cancer and normal gene expression profiling and interactive analyses. Nucleic Acids Res 45: W98-W102, 2017.

29. Hendrix ND, Wu R, Kuick R, Schwartz DR, Fearon ER and Cho KR: Fibroblast growth factor 9 has oncogenic activity and is a downstream target of Wnt signaling in ovarian endometrioid adenocarcinomas. Cancer Res 66: 1354-1362, 2006.

30. Bowen NJ, Walker LD, Matyunina LV, Logani S, Totten KA, Benigno BB and McDonald JF: Gene expression profiling supports the hypothesis that human ovarian surface epithelia are multipotent and capable of serving as ovarian cancer initiating cells. BMC Med Genomics 2: 71, 2009.

31. Elgaaen BV, Olstad OK, Sandvik L, Odegaard E, Sauer T, Staff AC and Gautvik KM: ZNF385B and VEGFA are strongly differentially expressed in serous ovarian carcinomas and correlate with survival. PLoS One 7: e46317, 2012.

32. Ahmed AA, Mills AD, Ibrahim AE, Temple J, Blenkiron C, Vias M, Massie CE, Iyer NG, McGeoch A, Crawford R, *et al*: The extracellular matrix protein TGFBI induces microtubule stabilization and sensitizes ovarian cancers to paclitaxel. Cancer Cell 12: 514-527, 2007.

33. Bushnell B: BBMap.https://sourceforge.net/projects/bbmap/. Accessed June 17, 2022.

34. Andrews S: FastQC: A quality control tool for high throughput sequence data. Available online. Retrieved May 17: 2018, 2010.

35. Dobin A, Davis CA, Schlesinger F, Drenkow J, Zaleski C, Jha S, Batut P, Chaisson M and Gingeras TR: STAR: Ultrafast universal RNA-seq aligner. Bioinformatics 29: 15-21, 2013.

36. Anders S, Pyl PT and Huber W: HTSeq-a Python framework to work with high-throughput sequencing data. Bioinformatics 31: 166-169, 2015.

37. Love MI, Huber W and Anders S: Moderated estimation of fold change and dispersion for RNA-seq data with DESeq2. Genome Biol 15: 550, 2014.

38. Bast RC Jr, Feeney M, Lazarus H, Nadler LM, Colvin RB and Knapp RC: Reactivity of a monoclonal antibody with human ovarian carcinoma. J Clin Invest 68: 1331-1337, 1981.

39. Yu-Rice Y, Edassery SL, Urban N, Hellstrom I, Hellstrom KE, Deng Y, Li Y and Luborsky JL: Selenium-Binding Protein 1 (SBP1) autoantibodies in ovarian disorders and ovarian cancer. Reproduction 153: 277-284, 2017.

40. Shin HY, Yang W, Lee EJ, Han GH, Cho H, Chay DB and Kim JH: Establishment of five immortalized human ovarian surface epithelial cell lines via SV40 T antigen or HPV E6/E7 expression. PLoS One 13: e0205297, 2018.

41. Hothorn T and Lausen B: Maximally selected rank statistics in R. R News 2: 3-5, 2002.

42. Li X, Li H, Yang C, Liu L, Deng S and Li M: Comprehensive analysis of ATP6V1s family members in renal clear cell carcinoma with prognostic values. Front Oncol 10: 567970, 2020.

43. Counis MF and Torriglia A: Acid DNases and their interest among apoptotic endonucleases. Biochimie 88: 1851-1858, 2006.

44. Martinez-Zaguilan R, Lynch RM, Martinez GM and Gillies RJ: Vacuolar-type H (+)-ATPases are functionally expressed in plasma membranes of human tumor cells. Am J Physiol 265: C1015-C1029, 1993.

45. Barar J and Omidi Y: Dysregulated pH in tumor microenvironment checkmates cancer therapy. Bioimpacts 3: 149-162, 2013.

46. Hong J, Yokomakura A, Nakano Y, Ishihara K, Kaneda M, Onodera M, Nakahama K, Morita I, Niikura K, Ahn JW, *et al*: Inhibition of vacuolar-type (H+)-ATPase by the cytostatic macrolide apicularen A and its role in apicularen A-induced apoptosis in RAW 264.7 cells. FEBS Lett 580: 2723-2730, 2006.

47. Wojtkowiak JW, Rothberg JM, Kumar V, Schramm KJ, Haller E, Proemsey JB, Lloyd MC, Sloane BF and Gillied RJ: Chronic autophagy is a cellular adaptation to tumor acidic pH microenvironments. Cancer Res 72: 3938-3947, 2012.

48. McConnell M, Feng S, Chen W, Zhu G, Shen D, Ponnazhagan S, Deng L and Li YP: Osteoclast proton pump regulator Atp6v1c1 enhances breast cancer growth by activating the mTORC1 pathway and bone metastasis by increasing V-ATPase activity. Oncotarget 8: 47675-47690, 2017.

49. Chueca E, Apostolova N, Esplugues JV, García-González MA, Lanas Á and Piazuelo E: Proton pump inhibitors display antitumor effects in Barrett's adenocarcinoma cells. Front Pharmacol 7: 452, 2016.

50. Hinton A, Bond S and Forgac M: V-ATPase functions in normal and disease processes. Pflugers Arch 457: 589-598, 2009.

51. Ohta T, Numata M, Yagishita H, Futagami F, Tsukioka Y, Kitagawa H, Kayahara M, Nagakawa T, Miyazaki I, Yamamoto M, *et al*: Expression of 16 kDa proteolipid of vacuolar-type H(+)-ATPase in human pancreatic cancer. Br J Cancer 73: 1511-1517, 1996.

52. Chung C, Mader CC, Schmitz JC, Atladottir J, Fitchev P, Cornwell ML, Koleske AJ, Crawford SE and Gorelick F: The vacuolar-ATPase modulates matrix metalloproteinase isoforms in human pancreatic cancer. Lab Invest 91: 732-743, 2011.

53. Lu Q, Lu S, Huang L, Wang T, Wan Y, Zhou CX, Zhang C, Zhang Z and Li X: The expression of V-ATPase is associated with drug resistance and pathology of non-small-cell lung cancer. Diagn Pathol 8: 145, 2013.

54. García-García A, Pérez-Sayáns M, Rodríguez MJ, Antúnez-López J, Barros-Angueira F, Somoza-Martín M, Gándara-Rey JM and Aguirre-Urízar JM: Immunohistochemical localization of C1 subunit of V-ATPase (ATPase C1) in oral squamous cell cancer and normal oral mucosa. Biotech Histochem 87: 133-139, 2012.

55. Pérez-Sayáns M, Reboiras-López MD, Somoza-Martín JM, Barros-Angueira F, Diz PG, Rey JM and García-García A: Measurement of ATP6V1C1 expression in brush cytology samples as a diagnostic and prognostic marker in oral squamous cell carcinoma. Cancer Biol Ther 9: 1057-1064, 2010.

56. Kulshrestha A, Katara GK, Ibrahim S, Pamarthy S, Jaiswal MK, Sachs AG and Beaman KD: Vacuolar ATPase 'a2' isoform exhibits distinct cell surface accumulation and modulates matrix metalloproteinase activity in ovarian cancer. Oncotarget 6: 3797-3810, 2015.

57. Song T, Jeon HK, Hong JE, Choi JJ, Kim TJ, Choi CH, Bae DS, Kim BG and Lee JW: Proton pump inhibition enhances the cytotoxicity of paclitaxel in cervical cancer. Cancer Res Treat 49: 595-606, 2017.

58. Lim JH, Park JW, Kim MS, Park SK, Johnson RS and Chun YS: Bafilomycin induces the p21-mediated growth inhibition of cancer cells under hypoxic conditions by expressing hypoxia-inducible factor-1alpha. Mol Pharmacol 70: 1856-1865, 2006.
59. Webb BA, Chimenti M, Jacobson MP and Barber DL: Dysregulated pH: A perfect storm for cancer progression. Nat Rev Cancer 11: 671-677, 2011.
60. Rishi G, Huang G and Subramaniam VN: Cancer: The role of iron and ferroptosis. Int J Biochem Cell Biol 141: 106094, 2021.
61. Torti SV and Torti FM: Iron and cancer: More ore to be mined. Nat Rev Cancer 13: 342-355, 2013.
62. Couch JA, Yu YJ, Zhang Y, Tarrant JM, Fuji RN, Meilandt WJ, Solanoy H, Tong RK, Hoyte K, Luk W, et al: Addressing safety liabilities of TfR bispecific antibodies that cross the blood-brain barrier. Sci Transl Med 5: 183ra57, 2013.
63. Deng Z, Manz DH, Torti SV and Torti FM: Iron-responsive element-binding protein 2 plays an essential role in regulating prostate cancer cell growth. Oncotarget 8: 82231-82243, 2017.
64. Shen J, Sheng X, Chang Z, Wu Q, Wang S, Xuan Z, Li D, Wu Y, Shang Y, Kong X, et al: Iron metabolism regulates p53 signaling through direct heme-p53 interaction and modulation of p53 localization, stability, and function. Cell Rep 7: 180-193, 2014.
65. Falzone L, Scandurra G, Lombardo V, Gattuso G, Lavoro A, Distefano AB, Scibilia G and Scollo P: A multidisciplinary approach remains the best strategy to improve and strengthen the management of ovarian cancer (Review). Int J Oncol 59: 53, 2021.
66. Rojas V, Hirshfield KM, Ganesan S and Rodriguez-Rodriguez L: Molecular characterization of epithelial ovarian cancer: Implications for diagnosis and treatment. Int J Mol Sci 17: 2113, 2016.